

26. *Physical Conditions of Earthquake Faults as Deduced from Geodetic Data.*

By Keichi KASAHARA,

Earthquake Research Institute.

(Read July 15, 1958—Received September 30, 1958.)

Summary

Horizontal displacement of triangulation points around an earthquake fault provides valuable information about physical conditions of faulting. The writer applies his theory of a strike-slip fault to some actual cases for the purpose of finding their probable conditions, such as the depth, the magnitude of stress change in the fault plane, and the strain energy associated with the crustal deformations. The analysis is effected for the San Andreas fault, the Gôamura fault, the Tanna fault, the Imperial Valley fault, and the Fairview Peak fault, geodetic data of which have been reported in detail by several geophysicists.

It is proved that these faults are as deep as 6~15 km approximately, the San Andreas fault being the shallowest whereas the Gôamura fault and the Fairview Peak fault are the deepest. This tendency seems to be in good harmony with distribution of their focal depths which were determined seismometrically. The stress change and the total strain energy are also estimated as shown in Table 1, where the rigidity is assumed as 5×10^{11} c.g.s.. The agreement of the strain energy with that of seismic waves can be seen in the respective cases, which confirms the view that sudden occurrence of such a faulting is the immediate cause of the earthquake.

Another notable bit of information is also obtained from the triangulation data. Theory predicts antisymmetric distribution of v_0 (horizontal displacement of triangulation stations) on both sides of a fault. In the actual distribution of v_0 , however, this characteristic is more or less disturbed by overlapping of another type of deformation. Quantitative discussion of this effect leads us to a conclusion that it can be attributed to strain accumulation in the earth's crust which developed gradually before the earthquake.

1. Introduction

The significance of faulting as the immediate cause of a great earth-

quake was first pointed out by H. F. Reid when he proposed the elastic rebound theory¹⁾. This idea has attracted the notice of many seismologists, especially of those in the United States and Canada, who worked out laborious investigations of earthquake-generating mechanism on the basis of this hypothesis. Although Reid's model seemed to provide a reasonable explanation for the fundamental characteristics of a strike-slip fault, more detailed examination was necessary for its widespread acceptance.

The present writer conducted, in his previous papers, a study of the nature of earthquake origins, wherein he proposed an improvement of the model²⁾. It is proved theoretically that this model provides more reasonable explanation for the crustal deformation which appears around the fault. Applying the theory to the actual geodetic data, we are able to estimate the probable conditions of the fault, such as the depth, the stress change in the fault plane, and the total strain energy.

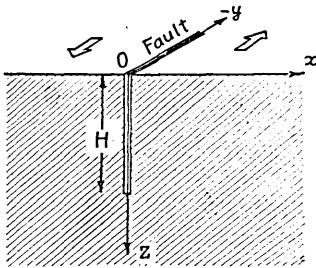


Fig. 1. Fault origin model of earthquakes.

The similar model has also been investigated by L. Knopoff, recently³⁾. With the aid of theory of electrostatic field he showed an exact solution for the problem, with which the writer's results agreed practically. P. Byerly and DeNoyer have presented another theory of crustal deformation for the purpose of estimating the depth and the energy of some earthquake faults⁴⁾. Their model assumes constant amplitude of deformation with depth, which is different from the one taken by Knopoff and the writer.

On the basis of these theories we are, now, able to discuss physical conditions of an earthquake fault, provided it is of strike-slip type and the deformation around it is known in detail by precise geodetic means.

Accumulation of this sort of knowledge would be very useful for further investigations of the mechanism of great earthquakes, so the writer intends to study more examples, to which the fault model is applicable.

1) H. F. REID, *Bull. Dept. Geol. Sci., Univ. California*, **6** (1911), 413-444.

2) K. KASAHARA, *Bull. Earthq. Res. Inst.*, **35** (1957), 473-532; *ibid.*, **36** (1958), 21-53. *Journ. Phys. Earth*, **6** (1958), 15-22.

3) L. KNOPOFF, *Geophys. Journ. R.A.S.*, **1** (1958), 44-52.

4) P. BYERLY and J. DENOYER, *Contributions in Geophysics in Honor of Beno Gutenberg* (1958), 17-35.

2. Method of analysis

The method of the following analysis is based on the fault model which has been presented previously⁵⁾. It is assumed that the earth's crust (homogeneous and perfectly elastic) is subject to a uniform shear stress, which increases with time and causes a fracture plane when it exceeds the strength of the medium. We also assume that the fracture is represented by a vertical plane of infinite length and of finite depth, in which the initial shear stress is liberated (Fig. 1). With the aid of the theory of elasticity, we calculate mathematically the deformation which is to be observed after the fracture. Fig. 2 illustrates the distribution of v_0 (displacement of a point at the earth's surface) diminishing with distance from the fault, in which the depth of the fault (H) is taken as a parameter.

These curves indicate that the earth's deformation predominates only in the limited regions lying on both sides of the fault and that the greater the value of H is, the wider the region of deformation becomes. Such a tendency being in good harmony with some of the observational data, we are able to find out the most probable value of H from their comparison. The theory also provides a way to compute the stress change in the fracture plane, $(Y_x)_0$, and the total amount of strain energy, E_f , as the functions of H , L , μ , v_{00} , where these symbols denote, respectively, the depth, the half-length of the actual fault, the rigidity of the crust, and the value of v_0 at the fault trace.

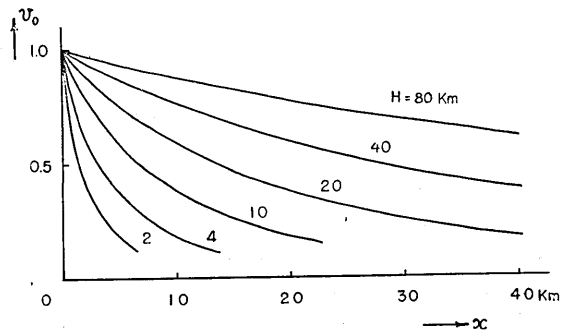


Fig. 2. Diminution curves of v_0 with distance from the fault (x).

3. Data used in the analysis

The following analysis is carried out for the cases of the California earthquake (1906), the Tango earthquake (1927), the North-Izu earthquake (1930), the Imperial Valley earthquake (1940), and the Fairview

5) *loc. cit.*, 2).

Peak earthquake (1954), all of which are accompanied by strike-slip faults. Descriptions of the first three cases have already been given in the previous papers, so that the following description is given only of the last two, which are newly added to our discussion.

The Imperial Valley fault (1940)

A great earthquake took place on May 18, 1940 in the Imperial Valley, California. This earthquake was accompanied by a long fault which was traceable across the epicentral area. Resurvey of the triangulation network over the area was carried out after the earthquake by the Coast and Geodetic Survey, which found out that the stations on the west side of the fault were shifted to northwest whereas those on the east side were shifted to the opposite direction⁶⁾. Lack of triangulation data in the area lying behind the border makes it impossible to get complete knowledge about the deformation. However, geological survey proves that the

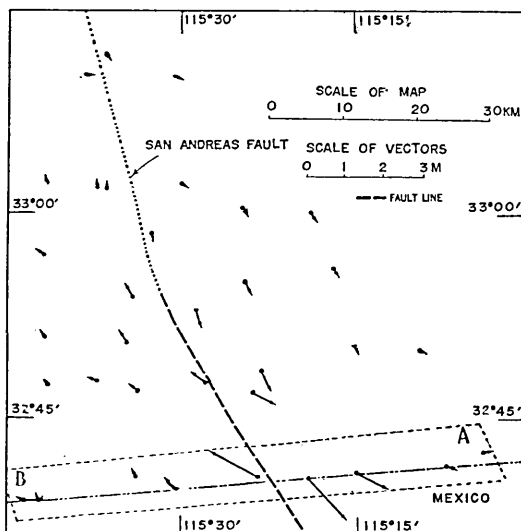


Fig. 3. Movements of triangulation stations around the Imperial Valley fault (after C. A. Whitten).

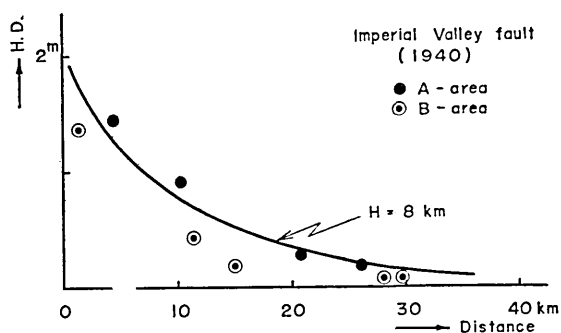


Fig. 4. Diminution curve of v_0 in the Imperial Valley area.

fracture extended to several tens of kilometres south of the border. Taking this fact into account, we assume that movements of the triangulation stations along the border line represent the most predominant part of the deformation. On this assumption, we plot the amplitudes of displacement

6) C. A. WHITTEN, *Journ. Coast and Geodetic Survey*, 2 (1949), 84-88.

Table 1. Physical Conditions of Earthquake Faults*)

Name	Main Shock					Fault					Remarks	
	Date	Epicentre	Depth	M	E_s	$\%_{00}$	2L	H	2L/H	(Y_z) ₀		E_f
San Andreas	1906 IV 18	38°N 123°W	Shallow	8 ¹ / ₄	ergs 2×10^{24}	m 2.5	km 440	km 6	73	c.g.s. 2.8×10^8	ergs 3×10^{24}	H=3.2 km (KNOFOFF) H=10 km (BYERLY & DENoyer)
Gómura	1927 III 7	35.6°N 135.2°E	10 km	7.5	10^{23}	1.5	30	15	2	5×10^7	4×10^{22}	
Tanna	1930 XI 26	35.1°N 139.0°E	0~5	7.0	2×10^{22}	2.0	15	8	2	1.2×10^8	3×10^{22}	
Imperial Valley	1940 V 18	32.7°N 115.5°W	Shallow	6.7	10^{22}	2.1	70	8	10	1.3×10^8	1.5×10^{23}	H=12 km (BYERLY & DENoyer)
Fairview Peak	1954 XII 16	35.2°N 118.1°W	15	7.4	6×10^{22}	1.5	60	15	4	5×10^7	7×10^{22}	H=23 km (BYERLY & DENoyer)

(μ is assumed as 5×10^{11} c.g.s.)

*) Numerical values of some items are corrected when they are reproduced from the previous papers. However, such correction is not so remarkable as to cause great alteration of the previous conclusions.

vectors for the eleven stations mentioned in Fig. 4, where data from both sides of the fault are plotted in the same coordinates. Applying the theoretical curves to them, we know that the most probable values of H and v_{00} are as follows.

$$H=8 \text{ km, and } v_{00}=200 \text{ cm.}$$

This estimation enables us, then, to compute $(Y_x)_0$ and E_f for the present case, the results of which are shown in Table 1.

The Fairview Peak fault (1954)

Two great earthquakes took place on December 16, 1954 in the Dixie Valley-Fairview Peak area of Nevada. They were accompanied by two major faults which appeared on the side of Fairview Peak and in Dixie Valley, respectively. Since the former one was the most conspicuous, the following discussion deals only with it.

Numbers of minor fractures appearing along the Fairview Peak fault made it difficult to determine the direction of the principal fault plane by geological survey. However, a seismometrical study conducted by C. Romney has concluded that one of the nodal planes lies in the direction of $N11^\circ W$ dipping 62° to east⁷⁾. This value being in good harmony with the direction of earth movements near the fault, we assume here that it represents the strike of the actual fault plane (see the chain line in Fig. 5). Triangulations prepared before and after the earthquake

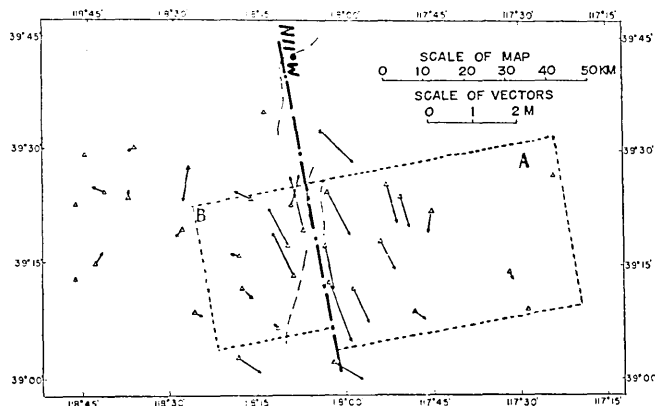


Fig. 5. Movements of triangulation stations around the Fairview Peak fault (after C. A. Whitten).

7) C. ROMNEY, *Bull. Seis. Soc. Amer.*, **47** (1957), 301-320.

by the Coast and Geodetic Survey have clarified the features of the deformation associated with the fault⁸⁾. Geodetic observations as well as the seismometrical solution for this fault indicated that the movement in the vertical direction was half of the horizontal one. So that it is not a strike-slip fault in the strict sense, however a tentative application of the theory of a strike-slip fault might be allowed in the present step of approximation.

The amplitudes of displacement vectors for the triangulation stations in A and B areas (see Fig. 5) are plotted against the distance, from which we find out that the diminution of v_0 can be explained by taking $H=15$ km and $v_{00}=150$ cm (Fig. 6). (Y_{x0}) and E_f are computed, then, as shown in Table 1.

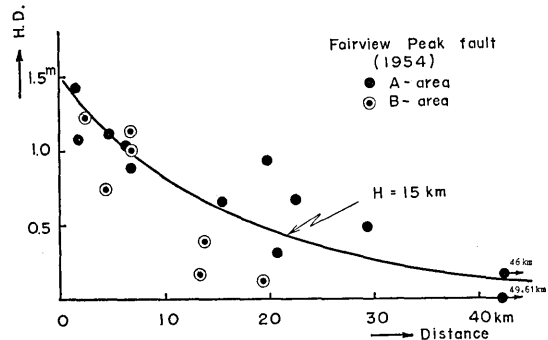


Fig. 6. Diminution curve of v_0 in the Fairview Peak area.

4. Faulting and elastic drift in the earth's crust.

The results of the foregoing analysis are compiled in Table 1, in which the conditions of the main shocks are also given for the sake of comparison. We notice, first, the relation between the depth of the seismic focus and of the fault plane. The present writer found out, previously, that the focus of the Tango earthquake was located at the lower part of the Gôamura fault. Such a relation is likely to hold good in all of the present cases. This fact is of essential meaning for the elastic rebound theory of earthquakes, which premises the spatial coincidence of the earthquake origin with the fault plane.

From the table we know that the aspect ratio of the faults ($2L/H$) differs much from each other, in which we notice, however, that the ratios for the faults in California are estimated at larger values than those for the others. D. Tocher, who investigated ground breakages in California and Nevada, expressed a view that the volume of elastic strain was no thicker for the largest shocks than it is for the smallest shock that produced a fault⁹⁾. The writer would not like here to check this only with the above-mentioned data, but he considers that it is

8) C. A. WHITTEN, *Trans. Amer. Geophys. Union*, **37** (1956), 393-398.

9) D. TOCHER, *Bull. Seis. Soc. Amer.*, **48** (1958), 147-153.

worth examining how H or $2L/H$ depends on the local conditions, by taking more examples.

$(Y_x)_0$ distributes in a range between 5×10^7 and 3×10^8 c.g.s.. From the viewpoint of our model, this quantity should be understood as the strength of the medium. C. Tsuboi has concluded, from another standpoint, that the ultimate strain of the earth's crust is about 10^{-4} .¹⁰⁾ After rough estimation by taking $\mu = 5 \times 10^{11}$ c.g.s., we see that the above-mentioned values of $(Y_x)_0$ harmonize well with Tsuboi's conclusion.

We also notice that the strain energy is estimated at the value nearly equal to that of seismic waves, in respective cases. This fact confirms the possibility that the energy source of an earthquake is the fault movement, provided it occurs in a very short time. Both sorts of energy being computed after rough approximation, more detailed investigation would be necessary for decisive conclusion. However, as long as we regard the estimation as order-of-magnitude one, the above-mentioned view can be accepted.

The theory predicts that the diminution curves on both sides of a fault are antisymmetric with one another. This prediction is likely to hold good in such a case as the Imperial Valley fault; however, in the case of the San Andreas fault, for instance, we see some distortion of the curves. The curve for the east side area approaches zero with distance, whereas that for the west side one ap-

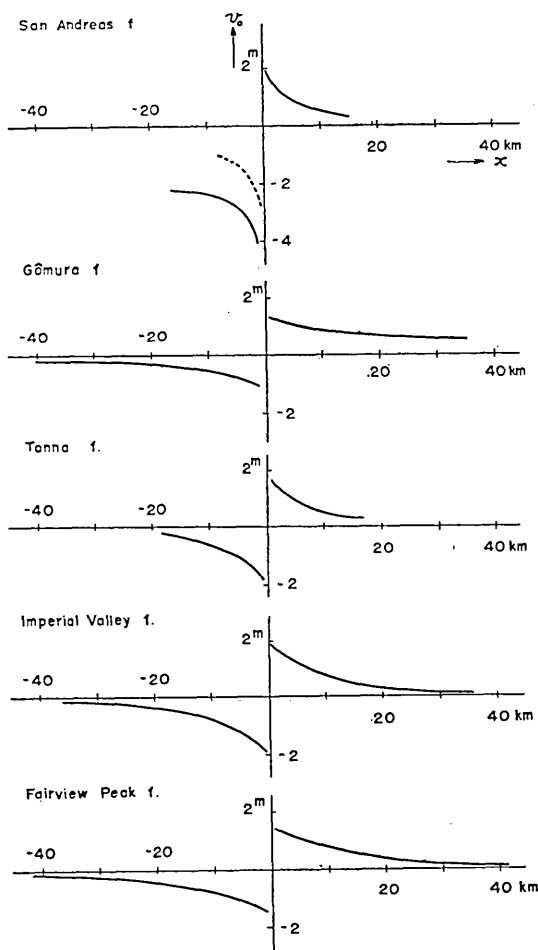


Fig. 7. Diminution curves (schematic).

proaches zero with distance, whereas that for the west side one ap-

10) C. Tsuboi, *Journ. Phys. Earth*, 4 (1956), 63-66.

proaches a certain finite value of v_0 , 200 cm say. This type of distortion can be seen, more or less, in the other cases as shown in Fig. 7, which might be attributed to the strain accumulation in the crust developed before the earthquake. In order to ascertain this supposition, we plot,

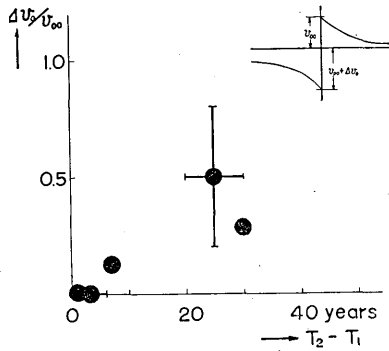


Fig. 8. Distortion of diminution curves versus time interval between the surveys.

in Fig. 8, the magnitude of distortion ($\Delta v_0/v_{00}$) against the time interval between the surveys conducted before and after the earthquake ($T_2 - T_1$). Suppose the distortion is caused by an elastic drift in the earth which overlaps the antisymmetric curves for the fault breakage, it is expected that the longer the time interval is, the more remarkable the distortion appears. The result in Fig. 8 confirms this supposition. The writer would like here to mention another important fact which proves more directly the elastic drift in the California district.

Geodetic triangulation prepared by C. A. Whitten has clearly indicated the drift of triangulation stations developing at a constant rate¹¹⁾. Taking this fact as well as the result of Fig. 8 into consideration, we might accept the reality of strain accumulation in the other districts, too.

5. Conclusions and acknowledgement.

The writer applied his theory of a strike-slip fault to five representative cases and estimated their physical conditions of faulting as shown in Table 1. The conclusions which are obtained from the present analysis are as follows.

1. The depths, to which the fault planes appeared from the earth's surface, are estimated at the values between 6 km and 15 km. They are nearly equal to the focal depths of the respective shocks.
2. The stress changes amounting to $5 \times 10^7 \sim 3 \times 10^8$ c.g.s. took place in the fracture planes. These values agree well with the strength of the crust, that has been concluded from another point of view.
3. The energy of crustal deformation and that of seismic waves are of the same order, in the respective cases.
4. The diminution curves of deformation indicate some distortion

11) C. A. WHITTEN, *loc. cit.*, 8).

due to the elastic drift in the earth's crust. The longer the time interval between the surveys before and after the earthquake is, the more remarkable the distortion becomes.

These results are likely to confirm the view that the faultings were the immediate causes of the respective earthquakes; however, a definite conclusion will be postponed until all the necessary examinations are carried out.

The writer wishes to acknowledge his hearty thanks to Dr. C. A. Whitten of the United States Coast and Geodetic Survey, who kindly offered the triangulation data for the present analysis. His thanks are also due to Miss R. Iwaya for her kind help in preparing the manuscript.

26. 地震断層の性状について

地震研究所 笠原慶一

さきに提出した断層模型の立場から、代表的な横切り断層と思われる San Andreas 断層、郷村断層、丹那断層（以上の 3 例については一部報告済み）、Imperial Valley 断層、Fairview Peak 断層についてその性状を考察した。おもな結論は次の通りである。

1. これらの断層面はそれぞれ 6 km から 15 km の深さに達していたものと推定されるが、験震学的に求められている震源の深さもまた、ほぼこれに匹敵する。
2. 断層面上の shear 歪力の変化は 5×10^7 c.g.s. から 3×10^8 c.g.s. の間に求められる。これは地殻の力学的強さに関する従来の常識から見ても妥当な数値と思われる。
3. 地殻変動の歪エネルギーと地震波動のエネルギーとは、それぞれの場合において同じ order であることが判つた。
4. 断層両側における水平変動の分布は逆対称であることが予想されるが、取扱つた実例のうちには分布曲線にある種の歪みが認められるものもある。この歪みの程度は、最初の測量から地震に至るまでの期間が長かつた場合ほど顕著であつて、地震前に地殻歪みが進行していた事実を裏書きするものと思われる。

以上の結果はいずれも断層地震説を主張する上に都合のよい事実であるが、単にこれだけの資料から決定的な議論はできない。更に地震学的その他の立場から検討を加える必要がある。